2.4 2-D Scattering by a graded-index dielectric circular cylinder

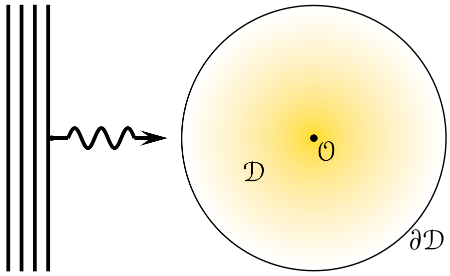

Figure 5: A time-harmonic incident plane wave illuminating a graded-index dielectric circular cylinder.

This is the first of two dielectric cylinder scattering problems. In both cases, the cylinder is aligned with the z-axis. We employ both cartesian coordinates $\{x, y, z\}$, and cylindrical polar coordinates $\{\rho, \varphi, z\}$.
Here, we shall consider a graded-index dielectric circular cylinder that is illuminated by a time-harmonic ($\exp(\mathrm{j}\omega t)$ time convention) incident plane wave $\boldsymbol{E} = E_0 \hat{\boldsymbol{z}}\, e^{-\mathrm{j}kx} = E_0 \hat{\boldsymbol{z}}\, e^{\mathrm{j}k\rho\cos(\varphi-\varphi_\mathrm{i})}$ with $\varphi_\mathrm{i} = \pi$ (or 180° if you prefer).
The invariance of both configuration and excitation with respect to z means that $\partial_z = 0$, which implies that Maxwell's equations indeed decouple into two sets of equations for two decoupled polarised states. In the transverse magnetic (TM_z) case, E_z, H_φ and H_ρ are the only non-vanishing field components.[2] Further, $H_\rho = (\mathrm{j}\omega\mu\rho)^{-1}\partial_\varphi E_z$, leaving a system of two coupled first-order partial differential equations for E_z and H_φ.
The cylinder has radius a, and a relative permittivity profile $\varepsilon_\mathrm{r} = n^2(\rho)$, where where n denotes the index of refraction (or refractive index). In addition to the invariance of configuration and excitation with respect to the z-direction, the configuration considered in this assignment is also axisymmetric (n is independent of φ). The configuration invariance in both z and φ implies that the remaining system of equations decouples, i.e., for each angular harmonic in cylindrical polar coordinates $\exp(\mathrm{j}m\varphi)$, we are left with a system of first-order ordinary differential equations for E_z and H_φ in the ρ-direction, which can be solved in terms of field constituents that

- satisfy the boundary conditions across $\rho = a$,
- remain bounded for $\rho \downarrow 0$
- outside the cylinder are associated with a scattered field that radiates away from the cylinder.

For the angular harmonic expansion of the incident field we use a Bessel summation theorem

$$e^{-\mathrm{j}k\rho\cos(\varphi)} = \sum_{m=-\infty}^{\infty} e^{\mathrm{j}m\varphi}(-\mathrm{j})^m J_m(k_1\rho), \tag{3}$$

where $k_1 = \omega\sqrt{\mu_1\varepsilon_1} = \omega n_1$ denotes the wavenumber in the homogeneous exterior domain.

2.4.1 Your mission, should you choose to accept it

Let us break down the assignment in a few logical steps.

1. For a lossless homogeneous dielectric cylinder with radius $a = \lambda$ and relative permittivity $n^2 = n_2^2 = 2$, embedded in vacuum ($n_1^2 = 1$), implement the expansion given in Appendix A, and share this reference solution with the team that will implement a FEM-BEM code for dielectric cylinders. This will help you (and the other team) in validating your codes.

[2]The subscript z clarifies that the magnetic field is transverse with respect to the symmetry direction z, i.e., $H_z = 0$.

Figure 6: Left: homogeneous dielectric circular cylinder. Right: coated PEC circular cylinder.

2. In preparation of the graded-index case, let us look at a coated PEC cylinder. The PEC cylinder has radius $b = \lambda$, and is surrounded coating of radius $a = 3\lambda/2$. Firstly, solve for the fields analytically. Secondly, integrate the system of ODEs numerically from $\rho = b$ to $\rho = a$, and apply the boundary conditions. Thirdly, validate your results *vis-a-vis* one of the reference problems in the FEM-BEM paper [2] (Figure 6, with a and b interchanged). Hence, this will also help you (and the other team) in validating your codes.

3. Next consider a lossless graded-index dielectric cylinder with radius $a = 6\lambda$ and relative permittivity

$$\varepsilon_r = \begin{cases} n_1^2 & \text{for } \rho > a, \\ (n_2^2 - n_1^2)(1 - \rho^2/a^2) + n_1^2 & \text{for } \rho \le a, \end{cases} \tag{4}$$

where n_2 denotes the refractive index at the centre, and n_1 denotes the refractive index in the homogeneous exterior (vacuum). This is a 2D version of a so-called Lüneburg lens (LL) that (asymptotically for high frequencies) focuses an incoming plane wave to the single line that is just the translation of the axis onto the circularly cylindrical boundary along the direction of the incident plane wave.

Now, the system of ODEs for $\rho < a$ cannot be solved any more in terms of J_m and J'_m as we have done in Appendix A. Instead, you have to integrate the system of ODEs numerically. However, there is a problem for $\rho \downarrow 0$, which is a regular singular point. You will have to introduce auxiliary variables similar to those introduced in [1] (Section 8.3), albeit that in [1] the system of ODEs is more complex because the polarisations do not decouple because there the fields depend on z through a common factor $\exp(-\mathrm{j}k_z z)$.

4. Once you have solved this LL problem for $a = 6\lambda$, try to see whether you can still achieve this for $a = 24\lambda$, and try to compare the computational effort of the four-fold scaling.

5. Finally, let us consider a lossless homogeneous dielectric cylinder of radius $a = 6\lambda$, illuminated by a time-domain incident plane wave

$$\boldsymbol{E} = E_0 \hat{\boldsymbol{z}}\, \mathscr{R}(t - (x + 2a)/c_0) \tag{5}$$

where c_0 denotes the speed of light in vacuum and

$$\mathscr{R}(t) = \left(1 - \frac{1}{2}\omega_p^2 t^2\right) \exp\left(-\frac{1}{4}\omega_p^2 t^2\right), \tag{6}$$

$$R(\omega) = \frac{4\sqrt{\pi}\omega^2}{\omega_p^3} \exp\left(-\frac{\omega^2}{\omega_p^2}\right) \tag{7}$$

denote the so-called Ricker wavelet [3], and its frequency-domain counterpart[3] with centre angular frequency $\omega_p = 2\pi c_0/\lambda$. You can solve this problem in the frequency domain. The

[3]Oddly, the author of [3] used the factor $1/(2\pi)$ in the forward Fourier transform.

inverse (fast) Fourier transform then leads to a space-times domain wavefield in which you may be able to recognise a so-called whispering gallery mode [4,5] propagating (and decaying) along the surface region of a dielectric object.

2.4.2 Proposed input and output

The required input parameters have been defined above. The absolute and relative tolerances for the numerical integration of the ODEs should be set to 10^{-12}. An adaptive Adams method is usually the most accurate option. Try setting it to a lower setting of say 10^{-6} and report on the differences.

For Subproblem 1, we first want to see a (log-scale) plot of $|a_m^{\mathrm{r}}|$ as a function of m defined in Appendix A. As output for Subproblems 1 and 2, we would like to see σ/λ as a function of φ, where $\sigma = \lim_{\rho\to\infty} 2\pi\rho \boldsymbol{E}^2/E_0^2$ denotes the bistatic scattering width for TM_zpolarisation, and the convergence rates with regard to the number of angular harmonics. As output for the Lüneburg lens Subproblems 3 and 4, we would like to see a plot of $|\boldsymbol{E}|^2/E_0^2$ on the boundary of the cylinder as a function of $\varphi \in [-\pi, \pi]$. As output for the whispering gallery mode Subproblem 5, we would like to see a movie of $|\boldsymbol{E}|^2/E_0^2$ on the boundary of the cylinder as a function of $\varphi \in [-\pi, \pi]$ (and time $t \in [0, 200]$fs, for a centre wavelength $\lambda_p = 1.55\,\mu\text{m}$.

2.4.3 Literature

[1] B. P. de Hon and R. Orta, *Wavefield Representations*, Lecture notes, Eindhoven University of Technology, 2021.

[2] M. D. Deshpande, C. R. Cockrell, and C. J. Reddy, *Electromagnetic Scattering Analysis of Arbitrarily Shaped Material Cylinder by FEM-BEM Method*, NASA Technical Paper 3575, 1996.

[3] Y. Wang, “The Ricker wavelet and the Lambert W function”, *Geophysical Journal International*, 200 (1):111–115, 2014.

[4] C. Vassallo. *Optical Waveguide Concepts*, Elsevier Science Publishers B.V., Amsterdam, The Netherlands, 1991.

[5] E.F. Franchimon, K.R. Hiremath, R. Stoffer and M. Hammer, “Interaction of whispering gallery modes in integrated optical microring or microdisk circuits: hybrid coupled mode theory model”, *J. Opt. Soc. Am. B*, 30 (4):1048–1057, 2013

2.5 2-D Scattering by a dielectric elliptic cylinder

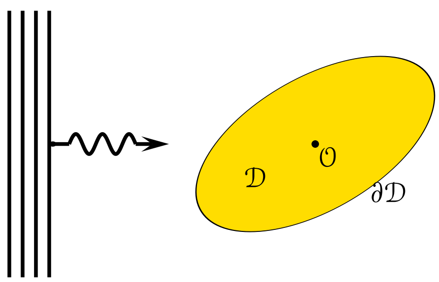

Figure 7: An elliptic dielectric cylinder illuminated by a time-harmonic incident plane wave.

This is the second of two dielectric cylinder scattering problems. In both cases, the cylinder is aligned with the z-axis. We employ both cartesian coordinates $\{x, y, z\}$, and cylindrical polar coordinates $\{\rho, \varphi, z\}$.